

Design and control of spin gates in two quantum dots arrays

Gonzalo Usaj and C. A. Balseiro

Instituto Balseiro and Centro Atómico Bariloche, Comisión Nacional de Energía Atómica, (8400) San Carlos de Bariloche, Argentina.

(Dated: October 27, 2018)

We study the spin-spin interaction between quantum dots coupled through a two dimensional electron gas with spin-orbit interaction. We show that the interplay between transverse electron focusing and spin-orbit coupling allows to dynamically change the *symmetry* of the effective spin-spin Hamiltonian. That is, the interaction can be changed from Ising-like to Heisenberg-like and vice versa. The sign and magnitude of the coupling constant can also be tuned.

PACS numbers: 73.63.Kv, 71.70.Gm, 73.23.Ad, 71.70.Ej

Coherent control and measurement of quantum spins are at the heart of new technologies with great potential value for information processing.^{1,2} This has led to a great activity in the field of quantum spin control in solid state devices.^{3,4,5,6,7,8,9,10} Since the seminal work by Loss and DiVincenzo,³ the exchange gate is the central tool underlying most of the proposals for spin manipulation in solid state devices based on quantum dots (QDs).^{4,5,6} The exchange gate is founded on the Heisenberg interaction between localized spins and so far nearly all implementations for such control are based on an ‘on/off’ setup—the interaction is either active or inactive. Furthermore, when the exchange gate is controlled by electrical gates, the control implies to ‘open’ or ‘close’ the QDs, changing their coupling to the environment, their shape and thus their detailed internal electronic structure. The question then is : Is it possible to engineer a predefined spin-spin interaction between QDs and then change its magnitude, sign and symmetry with a negligible impact on the internal structure of the dots?

In a recent work, we analyzed a way to tune the amplitude and sign of the spin coupling.¹¹ Here we go a step forward and show how to design a Heisenberg or an Ising-like interaction of the desired magnitude and sign of the coupling constant and then dynamically change one into the other by controlling a small magnetic field—the control mechanism relies on the interplay between transverse electron focusing and spin-orbit coupling.^{12,13,14,15} This opens up the possibility to manipulate spin-spin Hamiltonians in solid state devices as it is done today with NMR techniques in molecules.¹⁶

The setup consists of two QDs at the edges of two electron gases as schematically shown in Fig. 1a, with an interdot distance d of the order of $1\mu\text{m}$. Present semiconducting heterostructure technology allows tailoring this structure in two dimensional electron gases (2DEG). In the Coulomb blockade regime, the QDs can be gated to have an odd number of electrons so that they behave as magnetic objects. In what follows we describe them as localized $\frac{1}{2}$ spins. The virtual tunneling of electrons between the dots and the 2DEG leads to a Kondo coupling between the localized spins \vec{S}_i and the 2DEG spins described by the following Hamiltonian¹⁷:

$$\hat{H}_K = \sum_{i,\eta,\eta'} J_i \vec{S}_i \cdot \psi_{\eta\sigma}^\dagger(R_i) \frac{\vec{\sigma}_{\sigma\sigma'}}{2} \psi_{\eta'\sigma'}(R_i) \quad (1)$$

where $i = 1, 2$ indicates the left and right QD respectively,

$\psi_{\eta\sigma}^\dagger(R_i)$ creates an electron with spin σ in a Wannier-like orbital centered around the coordinate R_i of the i -th QD at the upper ($\eta = 1$) or lower ($\eta = 2$) plane. The spacial extension of the Wannier orbital depends on the opening of the QDs. This coupling leads to a RKKY-like interaction between the QDs spins that takes the general form¹⁸:

$$\hat{H}_J = -\frac{J_1 J_2}{4\pi} \text{Im} \int d\omega f(\omega) \text{Tr} \left(\vec{S}_1 \cdot \vec{\sigma} \mathbf{G}(1, 2) \vec{S}_2 \cdot \vec{\sigma} \mathbf{G}(2, 1) \right) \quad (2)$$

where $f(\omega)$ is the Fermi function and the 2×2 matrix $\mathbf{G}(i, j)$ is the Fourier transform of the retarded electron propagator whose elements are $G_{\sigma\sigma'}(i, j, t - t') = -i\theta(t - t') \times \sum_{\eta,\eta'} \langle \{ \psi_{\eta\sigma}(R_i, t), \psi_{\eta'\sigma'}^\dagger(R_j, t') \} \rangle$. When the electron’s spin is conserved along the electron propagation between QDs, $\mathbf{G}(i, j)$ is diagonal in the spin index and the spin-spin Hamiltonian (2) reduces to the Heisenberg one $\hat{H}_J = J \vec{S}_1 \cdot \vec{S}_2$ with the usual RKKY-like exchange $J = J_1 J_2 / 2\pi \text{Im} \int d\omega f(\omega) G_{\uparrow\uparrow}(1, 2) G_{\downarrow\downarrow}(2, 1)$.

The presence of a small magnetic field B_z perpendicular to the 2DEG creates edge states that dominate the electron scattering from objects placed at the 2DEG edges. The interaction between QDs is then mediated by these edge states and the propagators are mainly due to the semiclassical orbits shown in Figs. 1b and 1c. Due to the chiral nature of these orbits, the intra-plane scattering, described by the terms in Eq. (1) with $\eta = \eta'$, give forward scattering while the inter-plane terms (with $\eta \neq \eta'$) describe the backward scattering. Only the inter-plane backward scattering processes contribute to the effective interaction. In other words, each propagators in Eq. (2) is due to contributions from only one plane. As the external field increases the cyclotron radii of these orbits decrease: $r_c = \hbar k c / e B_z$ with k the electron wavevector. The focusing fields are those for which the interdot distance d is commensurate with the cyclotron radius r_c of electrons at the Fermi energy (E_F), that is $d = 2nr_c = 2n \hbar k_F c / e B_z$ with n an integer number. At the focusing fields, the electrons at the Fermi level scattered by one QD are focused onto the other leading to an amplification of the exchange integral J . The numerical result is shown in Fig. 1d where, for the sake of comparison with the conventional RKKY interaction, the exchange integral J is plotted as a function of the interdot distance for a fixed magnetic field. These results were obtained using a finite differences technique¹⁴ for a system with an effective electronic mass $m^* = 0.067m_e$ and $E_F = 5\text{meV}$, cor-

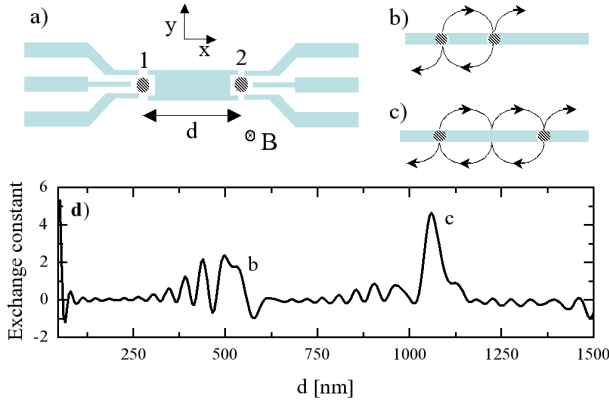


FIG. 1: **a)** Schematic view of the two QDs device. **b)** and **c)** illustrate the semiclassical orbits corresponding to the first and second focusing conditions, respectively. Arrows indicate the direction of motion. **d)** Exchange coupling constant J as a function of the interdot distance. A large value of J around the first (**b**) and second (**c**) focusing condition is clearly seen. The parameters correspond to a 2DEG with $m^* = 0.067m_e$ and $E_F = 5\text{meV}$. The magnetic field is $B_z = 227\text{mT}$ and the temperature is set to zero. The exchange constant is normalized to its value at $d \approx \lambda_F$, for $B_z = 0$ and without SO.

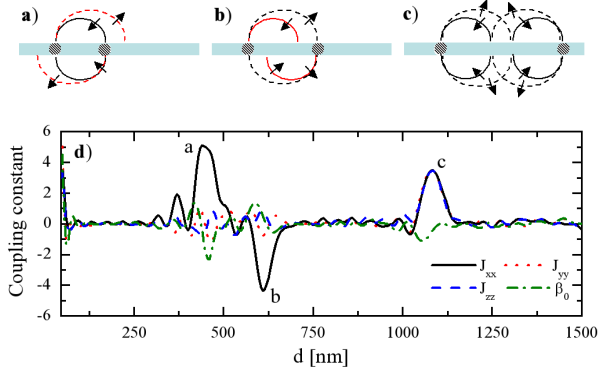


FIG. 2: Schematic representation of the first focusing condition for the smallest (**a**) and largest (**b**) cyclotron radius and of the second focusing condition (**c**) in the presence of SO coupling. The arrows indicate the spin orientation. In (**d**) the four coupling constants of Hamiltonian (4) are shown as a function of d . The SO parameter is taken to be $\alpha = 15\text{meVnm}$, and the other parameters as in Fig. 1.

responding to an electron density of $1.5 \times 10^{11}/\text{cm}^2$. With these parameters, the focusing amplification of the exchange integral is clearly observed. In the semiclassical picture, the first focusing condition ($n = 1$) corresponds to a direct propagation of the electrons from one QD to the other; in the second one ($n = 2$) the electron bounces once at the 2DEG edge. For interdot distances of the order of $1\mu\text{m}$, the magnetic fields for the first focusing conditions ($n = 1$ or 2) is small and neglecting the Zeeman spin splitting due to the external field is a good approximation. It is worth mentioning that, in similar geometries, the electron focusing due to small magnetic fields is clearly observed in transport experiments.^{7,12,19}

In systems with strong spin-orbit (SO) coupling, new effects arise. We consider a Rashba SO interaction in the 2DEG.^{20,21} This interaction is due to the inversion asymmetry of the confining potential and it is described by the Hamiltonian $H_{SO} = \alpha/\hbar(p_y\sigma_x - p_x\sigma_y)$ where p_γ are the components of the canonical momentum of the 2DEG electrons and σ_γ the spin operators. The SO coupling acts as a strong in-plane magnetic field proportional to the momentum. This breaks the spin degeneracy leading to two different conduction bands.²⁰

In the presence of a small magnetic field perpendicular to the gas plane, each band leads to a different cyclotron radius. These two radii manifest as two distinct focusing fields for the first ($n = 1$) focusing condition.¹⁴ This splitting has been observed by Rokhinson *et al.*¹⁵ in a p-doped GaAs/AlGaAs heterostructure. The spin texture of the orbits is such that, for small fields (large cyclotron radii), the electron's spin adiabatically rotates along the semiclassical orbit, being perpendicular to the momentum, as schematically shown in Fig. 2. In order to describe the magnetic scattering of electrons in this case, it is convenient to quantize the spin along the x -axis. Then, around the first focusing condition the propagators $G_{+,-}(i, j)$ and $G_{-,+}(i, j)$ dominate the interdot coupling, here the spin index \pm indicate the two spin projection. The interdot interaction is then approximately given by an Ising term $\hat{H}_I = J_{xx}S_{1x}S_{2x}$ with coupling constant given by

$$J_{xx} = \frac{J_1 J_2}{4\pi} \text{Im} \int d\omega f(\omega) G_{+,-}(i, j) G_{-,+}(j, i) \quad (3)$$

where $i = 1$ and $j = 2$ or $i = 2$ and $j = 1$ depending on which cyclotron radius contributes to the focusing. This result can be visualized in terms of the semiclassical trajectories shown in Figs. 2a and 2b: for a SO coupling strong enough to split the focusing condition, the inter-plane spin-flip backscattering mixes the two cyclotron radii living the electron out of the focusing condition. Thus, these spin-flip processes can not contribute to the coupling. The interdot interaction is then due to non-spin flip processes of electrons that are back-scattered. This defines the symmetry axis of the resulting Ising interaction.

At the second focusing condition, the system operates in a different way (see Fig. 2c). There are two important effects to consider: *i*) the orbits with different cyclotron radii are mixed at the bouncing point due to spin conservation, and *ii*) along the trajectories from one QD to the other the electron's spin completes a 2π rotation. As a consequence, the two orbits contribute to the exchange integral and $G_{+,+}(i, j)$ and $G_{-,-}(i, j)$ dominate the spin-spin coupling. In this way the rotational symmetric Heisenberg coupling is recovered.

For arbitrary external field, Hamiltonian (2) can be written as fully anisotropic Heisenberg model plus a Dzyaloshinski-Moriya term

$$\hat{H}_J = \sum_{\gamma} J_{\gamma\gamma} S_{1\gamma} S_{2\gamma} + \vec{\beta} \cdot (\vec{S}_1 \times \vec{S}_2) \quad (4)$$

where $\vec{\beta} = (0, \beta_0, 0)$. Hamiltonian (4) is a particular case of a more general Hamiltonian including SO effects.^{22,23,24} In our case, due to the symmetry of our geometry, there are only

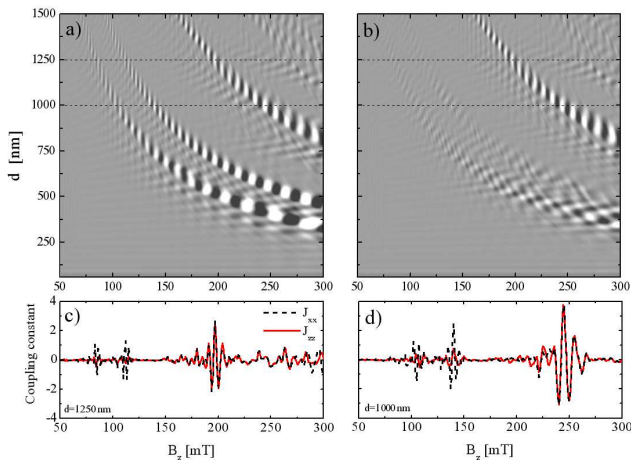


FIG. 3: The exchange constants J_{xx} (a) and J_{zz} (b) as a function of both the magnetic field B_z and the interdot distance d . Black (white) corresponds to large negative (positive) values of the exchange constants. Along the hyperbolas defined by the focusing conditions large amplitude oscillations are observed. The first focusing condition is split as explained in the text. (c) and (d) show slices taken at $d = 1\mu\text{m}$ in (c) and $d = 1.25\mu\text{m}$ in (d); J_{xx} and J_{zz} are shown with dashed and solid lines respectively. The isotropic nature of the exchange coupling at the second focusing condition is apparent. Parameters as in Figs. 1 and 2.

four independent parameters: $J_{\gamma\gamma}$ with $\gamma = x, y, z$ and β_0 . The numerical results for these coupling constants are shown in Fig. 2d. As argued above, around the first focusing condition the system behaves as an Ising like model: the dominant coupling J_{xx} shows a large amplification when the interdot distance matches each one of the two cyclotron orbits. The relative amplitude and sign of J_{xx} in these peaks depends on both the external field and the Fermi energy. At the second focus-

ing condition the system behaves as an isotropic Heisenberg model ($J_{xx} = J_{yy} = J_{zz}$) with a small anisotropic correction ($|\beta_0/J_{xx}| \ll 1$). Figures 3a and 3b show the dominant couplings, J_{xx} and J_{zz} respectively, as a function of B_z and d . The magnetic field not only can turn on and off each coupling but a fine tune around the focusing fields can change their sign too (see Figs. 3c and 3d).¹¹

There is a variety of systems that are potentially appropriate to observe these effects. While in n-doped GaAs/AlGaAs heterostructures the spin orbit is small, systems like p-doped GaAs/AlGaAs or InGaAs heterostructures present a large SO coupling. The nature of the SO effect depends on the system. Effects like the ones discussed in this work are also present in systems with Dresselhaus SO coupling. Furthermore, the external control of the relative magnitude of both contributions to the SO coupling,²⁵ could allow the control the quantization axis of the Ising-like interaction.

In summary, we have shown that the interplay between transverse electron focusing and spin orbit interaction gives a unique opportunity to control and tune the spin-spin interaction between QDs without inducing big changes in their internal structure. When the SO coupling is large, it leads to a spin-dependent focusing condition (for $n = 1$), resulting in a highly anisotropic Ising-like interaction. However, by doubling the external field a Heisenberg gate with a small correction of the Dzyaloshinski-Moriya type is recovered. In the context of quantum computing, there are strategies to eliminate or control these small corrections to the Heisenberg gate.^{24,26,27} The proposed setup can be extended to three or more QDs in a linear array. An array with different interdot distances and with extra gates used to blockade the focusing may be used to independently control the interdot interactions.

This work was partially supported by ANPCyT Grants No 13829 and 13476 and Fundación Antorchas, Grant 14169/21. GU acknowledge support from CONICET.

- ¹ D. Awschalom, N. Samarth, and D. Loss, eds., *Semiconductor Spintronics and Quantum Computation* (Springer, New York, 2002).
- ² M. A. Nielsen and I. L. Chuang, *Quantum Computation and Quantum Information* (Cambridge University Press, Cambridge, 2000).
- ³ D. Loss and D. P. DiVincenzo, *Phys. Rev. A* **57**, 120 (1998).
- ⁴ G. Burkard, D. Loss, and D. P. DiVincenzo, *Phys. Rev. B* **59**, 2070 (1999).
- ⁵ X. Hu and S. Das Sarma, *Phys. Rev. A* **61**, 062301 (2000).
- ⁶ D. P. Divincenzo, D. Bacon, J. Kempe, G. Burkard, and K. B. Whaley, *Nature* **408**, 339 (2000).
- ⁷ R. M. Potok, J. A. Folk, C. M. Marcus, and V. Umansky, *Phys. Rev. Lett.* **89**, 266602 (2002).
- ⁸ J. M. Elzerman, R. Hanson, J. S. Greidanus, L. H. W. van Beveren, S. D. Franceschi, L. M. K. Vandersypen, S. Tarucha, and L. P. Kouwenhoven, *Phys. Rev. Lett.* **67**, 161308 (2003).
- ⁹ Y. K. Kato, R. C. Myers, A. C. Gossard, and D. D. Awschalom, *Nature* **50**, 427 (2004).
- ¹⁰ Y. K. Kato, R. C. Myers, A. C. Gossard, and D. D. Awschalom, *Appl. Phys. Lett.* **86**, 162107 (2005).
- ¹¹ G. Usaj, P. Lustemberg, and C. A. Balseiro, *Phys. Rev. Lett.* **94**, 036803 (2005).
- ¹² H. van Houten, C. W. Beenakker, J. G. Williamson, M. E. I. Broekaart, P. H. M. Loosdrecht, B. J. van Wees, J. E. Mooji, C. T. Foxon, and J. J. Harris, *Phys. Rev. B* **39**, 8556 (1989).
- ¹³ C. W. Beenakker and H. van Houten, in *Solid State Physics*, edited by H. Eherenreich and D. Turnbull (Academic Press, Boston, 1991), vol. 44, pp. 1–228.
- ¹⁴ G. Usaj and C. A. Balseiro, *Phys. Rev. B* **70**, 041301(R) (2004).
- ¹⁵ L. P. Rokhinson, V. Larkina, Y. B. Lyanda-Geller, L. N. Pfeiffer, and K. W. West, *Phys. Rev. Lett.* **93**, 146601 (2004).
- ¹⁶ R. R. Ernst, G. Bodenhausen, and A. Wokaun, *Principles of Nuclear Magnetic Resonance in One and Two Dimensions* (Oxford, University Press, 1990).
- ¹⁷ R. Schrieffer and P. Wolf, *Phys. Rev.* **149**, 491 (1966).
- ¹⁸ H. Imamura, P. Bruno, and Y. Utsumi, *Phys. Rev. B* **69**, 121303 (2004).
- ¹⁹ J. A. Folk, R. M. Potok, C. M. Marcus, and V. Umansky, *Science* **299**, 679 (2003).
- ²⁰ E. I. Rashba, *Sov. Phys. Solid State* **2**, 1109 (1960).
- ²¹ Y. A. Bychkov and E. I. Rashba, *JETP Letters* **39**, 78 (1984).

- ²² I. Dzyaloshinski, *J. Phys. Chem. Solids* **4**, 241 (1958).
- ²³ T. Moriya, *Phys. Rep.* **120**, 91 (1960).
- ²⁴ N. E. Bonesteel, D. Stepanenko, and D. P. DiVincenzo, *Phys. Rev. Lett.* **87**, 207901 (2001).
- ²⁵ J. B. Miller, D. M. Zümbuhl, C. M. Marcus, Y. B. Lyanda-Geller, D. Goldhaber-Gordon, K. Campman, and A. C. Gossard, *Phys. Rev. Lett.* **90**, 076807 (2003).
- ²⁶ D. Stepanenko, N. E. Bonesteel, D. P. DiVincenzo, G. Burkard, and D. Loss, *Phys. Rev. B* **68**, 115306 (2003).
- ²⁷ D. Stepanenko and N. E. Bonesteel, *Phys. Rev. Lett.* **93**, 140501 (2004).